

# Dynamics of a Torsional System with Harmonically Varying Dry Friction Torque

Chengwu Duan<sup>1</sup> and Rajendra Singh

Acoustics and Dynamics Laboratory, Department of Mechanical Engineering, The Ohio State University, Columbus, Ohio 43210, USA.

E-mail: [duan.19@osu.edu](mailto:duan.19@osu.edu)

**Abstract.** Nonlinear dynamics of a single degree of freedom torsional system with dry friction is studied in this paper. First, the nonlinear system with a periodically varying normal load is formulated. Second, a multi-term harmonic balance method (MHBM) is re-formulated to directly solve the nonlinear time-varying problem in frequency domain. The feasibility of MHBM is demonstrated with a periodically varying friction and its accuracy is validated by numerical integration using Runge-Kutta scheme. Then, nonlinear frequency response is calculated by assuming classical Coulomb friction law under harmonically varying normal load. Effects of harmonic order and phase lag of normal load are then examined with the proposed approach. Our analysis shows that a change in the harmonic order of the normal load affects responses at both off-peak and peak frequencies while the phase lag has minimal influence on peak frequency responses.

## 1. Introduction

A classical single degree of freedom (SDOF) torsional system with dry friction element is shown in Figure 1. This system could be either nonlinear time-invariant (NLTI) or nonlinear time-varying (NLTV) type depending on the nature of applied normal load  $\bar{N}$ . The literature contains substantial work on time-invariant (NLTI) friction dynamics [1-4]. For example, Den Hartog pioneered the study of frequency response by assuming that the system would experience no more than two stops in one cycle [1]. Yet, time-varying normal load results from surface irregularity or contact fluctuation. Recently, Duan and Singh studied the influence of time-varying friction dynamics in a two degree of freedom system in which the friction element functions as a power transmission path as well [5]. However, our prior formulation was limited to a harmonically varying normal load and only the numerical integration method was employed that prevents detailed case studies. In this paper, we will overcome this deficiency by formulating a semi-analytical multi-term harmonic balance method and applying it to the nonlinear time-varying system (NLTV) problem. We will also analyze the effect of time-varying parameters on nonlinear frequency responses.

## 2. Problem Formulation

The SDOF torsional system is shown in Figure 1, with  $\bar{I}$  as moment of inertia,  $\bar{K}$  as torsional stiffness,  $\bar{C}$  as viscous damping term. Here,  $\bar{\theta}$  represents angular displacement. The dry friction

---

<sup>1</sup> To whom any correspondence should be addressed.

element is assumed to be subject to a periodically varying normal load  $\bar{N}(\bar{t})$ . Mathematically, this NLTV system can be described with equation (1).

$$\bar{I}\ddot{\bar{\theta}} + \bar{C}\dot{\bar{\theta}} + \bar{K}\bar{\theta} + \bar{T}_f(\dot{\bar{\theta}}, \bar{t}) = \bar{T}_p \sin(\bar{\omega}\bar{t}) \quad (1)$$

The nonlinear time-varying friction torque is given by speed-dependent friction coefficient  $\mu(\dot{\bar{\theta}})$ , effective arm of moment  $\bar{r}$  and  $\bar{N}(\bar{t})$  as:

$$\bar{T}_f(\dot{\bar{\theta}}, \bar{t}) = \bar{r}\mu(\dot{\bar{\theta}})\bar{N}(\bar{t}) \quad (2)$$

The normal load is assumed to be periodic with fundamental frequency  $\bar{\omega}/\kappa$  where  $\kappa$  is an integer. The dry friction is described by the classical Coulomb law though static and kinetic friction coefficients are assumed to be identical in this study.

$$\bar{N}(\bar{t}) = \bar{N}_0 + \sum_{n=1} \left( \bar{N}_{2n-1} \sin\left(\frac{n}{\kappa}\bar{\omega}\bar{t}\right) + \bar{N}_{2n} \sin\left(\frac{n}{\kappa}\bar{\omega}\bar{t}\right) \right), \quad (3a)$$

$$\bar{\mu}(\dot{\bar{\theta}}) = \begin{cases} \bar{\mu} & |\dot{\bar{\theta}}| > 0 \\ [-\bar{\mu} \quad \bar{\mu}] & |\dot{\bar{\theta}}| = 0 \end{cases} \quad (3b)$$

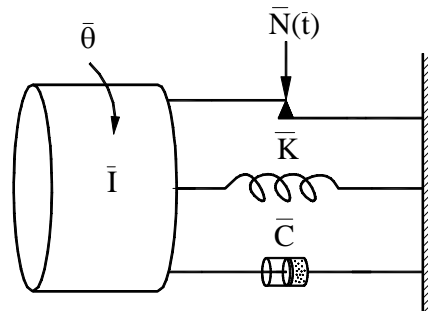


Figure 1 Example case: SDOF torsional, nonlinear time-varying (NLTV) system. This oscillator includes a dry friction element under periodically varying normal load  $\bar{N}(\bar{t})$

Equation (1) can be further simplified by introducing the following dimensionless parameters:

$$\bar{\omega}_n = \sqrt{\bar{K}/\bar{I}}, \quad \zeta = \bar{C}/(2\sqrt{\bar{K}\bar{I}}), \quad \bar{\theta}_c = \bar{T}_p/\bar{K}, \quad (4a-c)$$

$$\theta = \bar{\theta}/\bar{\theta}_c, \quad T_p = \bar{T}_p/\bar{T}_p = 1.0, \quad T_f = \bar{T}_f/\bar{T}_p, \quad (4d-f)$$

$$\Omega = \bar{\omega}/\bar{\omega}_n, \quad \tau = \bar{\omega}_n \bar{t}. \quad (4g-h)$$

Finally, the following dimensionless equation is obtained where  $(\cdot)' = d(\cdot)/d\tau$  and  $(\cdot)'' = d^2(\cdot)/d\tau^2$ .

$$\theta'' + 2\zeta\theta' + \theta + \underbrace{T_f(\theta', \tau)}_{\text{Nonlinear Time Varying Term}} = T_p \sin(\Omega\tau) \quad (5)$$

Chief objective of this paper is to study the nonlinear frequency response of the SDOF system. A multi-term harmonic balance method is re-formulated to solve the nonlinear time-varying (NLTV) system and directly calculate the response in frequency domain. As the simplest form of periodicity, the effect of harmonically varying normal load is studied. We will demonstrate the applicability of the multi-term harmonic balance method for this problem and validate its accuracy by comparing semi-analytical predictions with the results yielded by numerical integration.

### 3. Multi-Term Harmonic Balance Method (MHBM) for NLTV System

A multi-term harmonic balance method (MHBM) is applied to solve Eq. (5) and determine the periodic response of  $\theta(\tau)$ . Previous researchers have applied MHBM only to the NLTI systems [6-8]. Re-formulation is necessary before adapting it to the NLTV system. In this section, a generic formulation for the NLTV system is illustrated. Essentially, the MHBM constructs approximate periodic responses that are represented by a truncated Fourier series, as shown below, where  $N_h$  is the harmonic order and  $\nu$  is the sub-harmonic index. For the sake of illustration, the nonlinear term in (5) is further generalized as  $F_f(\theta, \dot{\theta}, t) = u(\theta)v(\dot{\theta})q(\tau)$ .

$$\theta(\tau) = a_0 + \sum_{n=1}^{N_h \nu} \left( a_{2n-1} \sin\left(\frac{n}{\nu} \Omega \tau\right) + a_{2n} \cos\left(\frac{n}{\nu} \Omega \tau\right) \right) \xrightarrow{\text{discretize}} \underline{\underline{\theta}} = \underline{\underline{\Delta a}} \quad (6a)$$

$$T_f = b_0 + \sum_{n=1}^{N_h \nu} \left( b_{2n-1} \sin\left(\frac{n}{\nu} \Omega \tau\right) + b_{2n} \cos\left(\frac{n}{\nu} \Omega \tau\right) \right) \xrightarrow{\text{discretize}} \underline{\underline{T_f}} = \underline{\underline{\Delta b}} \quad (6b)$$

Here,  $\underline{\underline{\Delta}}$  is the discrete inverse Fourier transform operator:

$$\underline{\underline{\Delta}} = \begin{bmatrix} 1 & \sin\left(\frac{n}{\nu} \Omega \tau_0\right) & \cos\left(\frac{n}{\nu} \Omega \tau_0\right) & \cdots & \cos\left(\frac{N_h \nu}{\nu} \Omega \tau_0\right) \\ \vdots & \vdots & \vdots & \vdots & \vdots \\ 1 & \sin\left(\frac{n}{\nu} \Omega \tau_{K-1}\right) & \cos\left(\frac{n}{\nu} \Omega \tau_{K-1}\right) & \cdots & \cos\left(\frac{N_h \nu}{\nu} \Omega \tau_{K-1}\right) \end{bmatrix} \quad (7)$$

Next, the numerical integration of Eq. (5) is transformed into an algebraic problem by matching the harmonic coefficients between the excitation (with coefficient  $T_p$  and denoted as  $\underline{\underline{p}}$  in vector format) and responses. Then numerical continuation or path following technique is employed to minimize the residue  $\underline{\underline{R}}$  where  $\underline{\underline{D}}$  is a differentiator and  $\underline{\underline{b}} = \underline{\underline{\Delta}}^+ T_f = (\underline{\underline{\Delta}}^T \underline{\underline{\Delta}})^{-1} \underline{\underline{\Delta}}^T T_f$ .

$$\underline{\underline{\Delta}} \left( \underline{\underline{R}} = \Omega^2 \underline{\underline{D}}^2 \underline{\underline{a}} + 2\zeta \Omega \underline{\underline{D}} \underline{\underline{a}} + \underline{\underline{a}} + \underline{\underline{b}} - \underline{\underline{p}} \right) \quad (8a)$$

Or,

$$\underline{\underline{R}} = \Omega^2 \underline{\underline{D}}^2 \underline{\underline{a}} + 2\zeta \Omega \underline{\underline{D}} \underline{\underline{a}} + \underline{\underline{a}} + \underline{\underline{b}} - \underline{\underline{p}} \quad (8b)$$

To ensure the minimization process following the deepest descent, Jacobian ( $\underline{\underline{J}}$ ) matrix has to be defined. (Readers should refer to [8] for a more detailed discussion of the MHBM.)

$$\underline{\underline{J}} = \frac{\partial \underline{\underline{R}}}{\partial \underline{\underline{a}}} = \Omega^2 \underline{\underline{D}}^2 + 2\zeta \Omega \underline{\underline{D}} + \frac{\partial \underline{\underline{a}}}{\partial \underline{\underline{a}}} + \frac{\partial \underline{\underline{b}}}{\partial \underline{\underline{a}}} \quad (9)$$

Since  $\theta$  is periodic,  $u(\theta)$  and  $v(\theta')$  are also periodic. In addition, the periodic  $q(\tau)$  can be expressed as  $\underline{q}(\tau) = \underline{\Delta} \underline{c}$ , since it is independent from  $\theta$  and  $\theta'$  and  $\underline{c}$  is usually a known vector. Consequently, the following  $\partial \underline{b} / \partial \underline{a}$  expression holds,

$$\frac{\partial \underline{b}}{\partial \underline{a}} = \left( \frac{\partial \underline{b}}{\partial \underline{T}_f} \right) \left[ \frac{\partial \underline{T}_f}{\partial \underline{\theta}} \frac{\partial \underline{\theta}}{\partial \underline{a}} + \frac{\partial \underline{T}_f}{\partial \underline{\theta}'} \frac{\partial \underline{\theta}'}{\partial \underline{a}} \right] \quad (10a)$$

$$\frac{\partial \underline{T}_f}{\partial \underline{\theta}} = \text{diag} [\underline{v}(\theta')] \text{diag} [\underline{q}(\tau)] \left[ \frac{\partial \underline{u}(\theta)}{\partial \underline{\theta}} \right], \quad \frac{\partial \underline{\theta}}{\partial \underline{a}} = \underline{\Delta} \quad (10b-c)$$

$$\frac{\partial \underline{T}_f}{\partial \underline{\theta}'} = \text{diag} [\underline{u}(\theta)] \text{diag} [\underline{q}(\tau)] \left[ \frac{\partial \underline{v}(\theta')}{\partial \underline{\theta}'} \right], \quad \frac{\partial \underline{\theta}'}{\partial \underline{a}} = \underline{\Omega} \underline{\Delta} \underline{D} \quad (10d-e)$$

Finally, the path following technique is used to calculate the turning points. The basic idea is to include  $\partial \underline{R} / \partial \underline{\Omega}$  as an independent vector and form an augmented  $\underline{J}$ .

$$\frac{\partial \underline{R}}{\partial \underline{\Omega}} = 2\underline{\Omega} \underline{D}^2 + 2\underline{\zeta} \underline{D} + \frac{\partial \underline{b}}{\partial \underline{\Omega}} \quad (11a)$$

$$\frac{\partial \underline{b}}{\partial \underline{\Omega}} = \frac{\partial \underline{b}}{\partial \underline{T}_f} \frac{\partial \underline{v}(\theta')}{\partial \underline{\theta}'} \frac{\partial \underline{\theta}'}{\partial \underline{\Omega}} \quad (11b)$$

To apply the above formulation to the problem of this paper, one should simply replace  $u(\theta)$  with an identity,  $v(\theta')$  with  $\mu(\theta')$  and  $q(\tau)$  with  $N(\tau)$ .

#### 4. Nonlinear Frequency Responses and Conclusion

First, the applicability of MHBMM is demonstrated. Figure 2 shows the nonlinear frequency responses of the system with a harmonically varying friction. Here,  $\underline{N}(\tau)$  is expressed by the following notation:  $\underline{N}(\tau) = \underline{\Delta} \underline{d}$  and  $\underline{d} = [0.6 \ 0.2 \ 0.1 \ 0.3 \ -0.5]^T$ . Clearly, the NLTV and NLTV systems responses differ significantly. For the sake of validation, numerical integration employing Runge-Kutta algorithm [9] is also carried out. As shown in Figure 2, an excellent match between MHBMM and numerical integration solutions is evident over the entire frequency range of interest. Next, to examine the effect of periodic varying normal load, we consider the simplest case by assuming a harmonic wave of  $\underline{N}(\tau)$  (with a dc term) though the MHBMM can also be used to examine a more general periodic normal load:

$$\underline{N}(\tau) = N_0 + N_1 \sin(n\Omega\tau) + N_2 \cos(n\Omega\tau) = N_0 + A \sin(n\Omega\tau + \phi), \quad (12a)$$

$$A = \sqrt{N_1^2 + N_2^2}, \quad \phi = \tan^{-1}(N_2 / N_1). \quad (12b-c)$$

By assuming zero phase  $\phi$  and the same  $A$ , the effect of harmonic order  $n$  is studied. As evident in Figure 3, a change in  $n$  affects the response over both low and high frequency regimes. Clearly,  $n=1$  has the highest response at higher frequency. The  $n=2$  term appears to suppress the vibration almost over the entire frequency range but it enhances the response at the peak frequency. Further, the

effect of  $n$  at lower frequency is rather mixed. For instance, the response curves for different  $n$  cross each other and no single  $n$  can claim the best attenuation effect. This is indeed different from the NLTI dry friction path problem [5] for which a clear pattern is recognized at lower frequencies though a mixed effect is seen at higher frequencies.

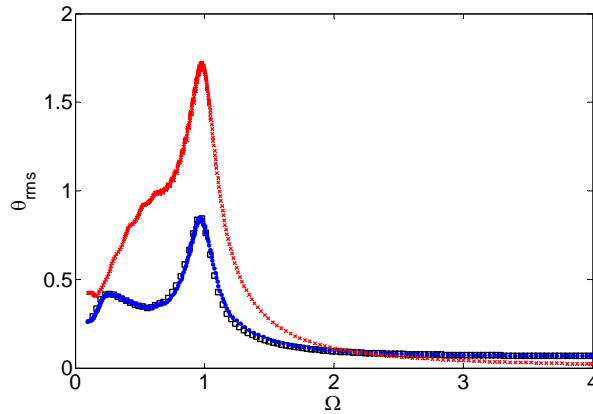


Figure 2 Nonlinear frequency responses of the NLTV and NLTI versions of the oscillator of Figure 1. Key:  $\times\times\times$ , NLTI using MHB;  $\bullet\bullet\bullet$ , NLTV using MHB;  $\square\square\square$ , NLTV using numerical integration.

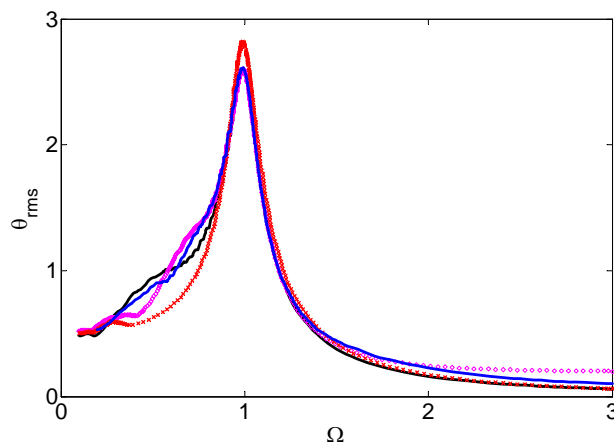


Figure 3 Effect of harmonic order ( $n$ ) of  $\underline{N}(\tau)$  on the frequency response, with  $N_0 = 0.5$ ,  $A = 0.3$  and  $\phi = 0$ . Key: —,  $n = 0$ ; - - -,  $n = 1/2$ ;  $\diamond\diamond$ ,  $n = 1$ ;  $\times\times\times$ ,  $n = 2$ .

Figure 4 presents the nonlinear ( $n = 1$ ) frequency responses for different  $\phi$  values. At first, it is interesting to note that a variation in  $\phi$  has minimal effect on the peak responses. By defining a pseudo lag  $\psi(\Omega)$  between the maximum response  $\theta(\tau)$  and the maximum excitation  $T_p(\tau)$ , we find that  $\psi$  tends to resemble the pattern of a classical linear time-invariant (LTI) SDOF system as  $\psi$  crosses  $\pi/2$  at resonance and is near  $\pi$  beyond the peak frequency. However,  $\psi(\Omega)$  differs significantly as a result of stick-slip motions in the lower frequency range. This explains different effects of  $\phi$  at lower and higher frequencies.

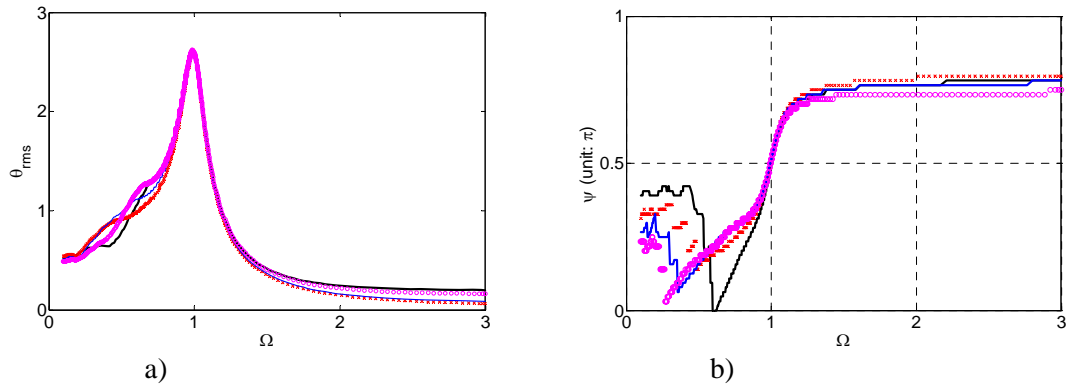


Figure 4 Effect of phase lag of  $N(\tau)$  on the nonlinear frequency responses, with  $N_0 = 0.5$ ,  $A = 0.3$  and  $n = 1$ . a) root mean square responses of  $\theta(\tau)$ ; b) mapping of pseudo lag  $\psi$ . Key: —,  $\phi = 0^\circ$ ;  $\times\times\times$ ,  $\phi = 60^\circ$ ; - - -,  $\phi = 90^\circ$ ;  $\circ\circ\circ$ ,  $\phi = 120^\circ$ .

#### References

- [1] Den Hartog 1931 *J P Trans. ASME APM* **53** 107
- [2] Pratt T K and Williams R 1981 *J. Sound. Vib.* **74** 531
- [3] Shaw S W 1986 *J. Sound. Vib.* **108** 305
- [4] Duan C and Singh R 2005 *J. Passenger Car* **116** 2785
- [5] Duan C and Singh R 2006 *J. Sound. Vib.* **294** 503
- [6] Von Groll G and Ewins D J 2001 *J. Sound. Vib.* **241** 223
- [7] Kim T C , Rook T E , and Singh R 2005 *J. Sound. Vib.* **281** 965
- [8] Duan C and Singh R 2005 *J. Sound. Vib.* **285** 803
- [9] Dormand J R and Prince P J 1980 *J. Comput. Appl. Math.* **6** 19